Properties of Silica with Zinc Oxide Nanocomposite and Its Antibacterial Effect

Christy Sandra Fernando B[1], N.S. Nirmala Jothi[2]

[1]Research Scholar, Department of Physics, Loyola College, Chennai
[2]Assistant Professor, Department of Physics, Loyola College, Chennai

Abstract
Nano-Silica is a versatile material which is obtained from agricultural sources and can be synthesized by chemical method in the laboratory. It is a low cost, environmentally friendly material. Zinc oxide is a type of metal oxide nanomaterial which can also be synthesized from plant sources and microorganisms, also by chemical methods. It is a highly useful material in biomedical applications. This research article highlights the potential of Silica with Zinc oxide Nanocomposite for inhibiting pathogenic bacteria, thus proving it has an effective antibacterial potential. Tetraethyl Orthosilicate (TEOS) was used as the precursor for synthesizing Nano-Silica. Zinc Acetate Dihydrate was used as the precursor to synthesize Zinc oxide. Nanocomposite of Silica with Zinc oxide was synthesized using one of the chemical methods of Nanotechnology called the “Hydrothermal” method. The prepared material was analyzed for its structural and morphological features by X-Ray Diffraction (XRD), Field Emission Scanning Electron Microscopy (FESEM), High-Resolution Transmission Electron Microscopy (HRTEM) and Selected Area Electron Diffraction (SAED). The elemental composition of the nanocomposite was analyzed by Energy Dispersive X-ray Analysis (EDAX). The functional groups present in the material was identified by Fourier Transform Infra-Red (FTIR) Spectroscopy and Fourier Transform Raman (FT Raman) Spectroscopy. The optical properties were analyzed from Ultraviolet-Visible (UV-Vis) Spectroscopy and Photoluminescence (PL) Spectroscopy. The surface charge of the material was determined from Zeta Potential measurement. The nanocomposite was tested against three gram-positive bacteria and seven gram-negative bacteria. The zone of inhibition of the bacteria by the nanocomposite was found.

Keywords: Nanomaterials, Silica, Zinc oxide, Antibacterial activity

1. Introduction
Metal oxide nanoparticles have gained significant attention due to its properties such as tunable size and porosity for suitable applications. Different metal oxides like zinc oxide, titanium dioxide, iron oxide, nickel oxide, copper oxide are synthesized in different shapes and structures and used in “biomedical applications” [1]. Metal oxides are prepared by chemical or biological method. The chemical method of synthesis is convenient to control the size and shape of nanomaterials, whereas the biological method is the production of metal oxides from plant extract, bacterial or fungal species. Both the methods are suitable for producing metal oxide nanoparticles for biomedical applications [2]. These metals and their oxides are suitable for targeting and inhibiting pathogenic microorganisms. These materials are also used in other medical and dental applications [3].

Silica nanoparticles are produced from chemical methods of nanotechnology such as sol-gel method, hydrothermal method, precipitation method or from agricultural sources such as corn cob, rice husk, wheat husk, bamboo leaves, paddy husk, sugarcane bagasse, etc. It is a non-carcinogenic material that occurs in amorphous and crystalline phases [4]. It is widely available in the crust of the Earth, which has applications in different fields including electronics, construction sector, medical field, etc. It acts as a "drug carrier" which can deliver drugs to the target site in the human body and used to diagnose and treat diseases including cancer [5]. The size and porosity of silica nanoparticles are controlled thus making it biologically compatible and useful for inhibiting harmful bacteria. Its large surface area makes it efficient to load and release drugs and aid to overcome the limitations of antibiotics which are less effective on bacteria [6]. Silica nanoparticles are functionalized by metal oxide nanomaterials for inhibition of different gram-positive and gram-negative bacteria. These nanocomposites are prepared in different shapes and sizes from plant-based materials and microorganisms to make it efficient for biomedical applications [7]. Silica nanoparticles are used in "targeted drug delivery" and "controlled release" of anti-cancer drugs. Nanomaterials can overcome the limitations of chemotherapy and radiotherapy such as damaging the normal tissues and side effects of radiation [8].

Zinc oxide nanoparticles are economical, non-toxic, highly stable, biologically compatible metal oxides efficient for medical field applications, sensor devices, electronics and communication systems and cytotoxicity against cancer cells. It is also known to efficiently inhibit bacterial growth [9]. Zinc oxide is synthesized by artificial physical or chemical methods in the laboratory, but it is considered "eco-friendly" when prepared from natural plant extracts of medicinal plants and microbial species. Zinc oxide nanoparticles are also useful in manufacturing of sensors, optoelectronic devices and solar cells [10]. Plant extracts can include any part of plants like roots, stem, leaves, flowers and fruits and microorganisms may include several bacteria, viruses and fungi. Some of the medical field applications of zinc oxide includes drug delivery to the targeted site of infection, cancer diagnosis and therapy, healing of wounds, and imaging techniques in biosensors [11]. Zinc oxide nanoparticles have antibacterial and anti-cancer properties. Common chemical precursors used in synthesizing zinc oxide include zinc acetate, zinc chloride, zinc sulphate and zinc chloride [12]. Zinc oxide nanomaterials at particular concentrations are proven to inhibit gram-positive bacteria. These are "inorganic" class of nanomaterials used in manufacturing cosmetics, drugs in pharmaceutical industries, packaging and additives in food industry [13]. They are effective in targeting microbial organisms, and proven useful to be used in manufacturing antibiotics for bacterial infections. Zinc oxide prepared with different morphologies and porosities has an effect on the inhibitory potential of microorganisms [14]. Zinc oxide nanoparticles are reliable and low-cost nanomaterials which has potential benefits in concrete manufacturing and also has "photocatalytic" applications. They are synthesized chemically by different top-down or bottom-up approaches of nanotechnology [15]. Nanostructures prepared from different methods produce materials in various shapes. Some of the citrus fruits are also sources for zinc oxide nanoparticles [16].

2. Materials and Methods

2.1 Materials

All the materials were purchased from Sigma Aldrich. Zinc acetate dihydrate – chemical precursor for zinc oxide, Tetraethyl orthosilicate (TEOS) – silica precursor, Cetyl Trimethyl Ammonium Bromide (CTAB) – a cationic surfactant and sodium hydroxide and Whatman Filter paper No.1 was used without further purification. Distilled water was obtained from the laboratory.

2.2 Preparation of Silica with Zinc oxide Nanocomposite

About 3-5 pellets of sodium hydroxide were stirred for 2 mins at 40 rpm with 20 ml H_2O and a clear aqueous solution with pH 14 was obtained. 1.5g CTAB was dissolved in 100 ml H_2O by stirring for 10 minutes at 40 rpm. 10 ml of TEOS [17] was added and stirred for 10 minutes. A clear solution of 0.5M Zinc acetate was prepared by dissolving 2.2g of zinc oxide precursor (Zinc acetate dihydrate) in 20 ml distilled water. It was stirred for 10 minutes and the pH was found to be 7.5. Few drops of sodium hydroxide were added and stirred for 15 minutes and the pH value was made to 10. The entire solution was simultaneously stirred and heated at 40°C for 2 hours. The solution was transferred to stainless steel Teflon lined autoclave and heated in a muffled furnace at 100°C for 8 hours. The liquid was then filtered using Whatman filter paper and taken in a petri dish. It was sealed with perforated parafilm, closed and kept in deep freezer at -20°C for 21 hours. The solid compound was lyophilized at -80°C for 7 hours by covering the petri dish with perforated aluminum foil. Finally, 4g sample was obtained [18]. Figure 1 shows the schematic diagram of the synthesis procedure of Silica with Zinc oxide Nanocomposite.

Figure 1: Synthesis Procedure Of Silica With Zinc Oxide

3. Results and Discussion

Silica nanoparticles were synthesized from its precursor Tetraethyl orthosilicate (TEOS), zinc oxide nanoparticles were synthesized from its precursor Zinc Acetate Dihydrate. Nanocomposite of silica with zinc oxide was prepared by following hydrothermal method of nanotechnology. Silica with Zinc oxide nanocomposite was studied for its structural features by X-Ray Diffraction (XRD), Field Emission Scanning Electron Microscopy (FESEM) and High-Resolution Transmission Electron Microscopy (HRTEM) and Selected Area Electron Diffraction (SAED). The elemental composition of the nanocomposite was analyzed by Energy Dispersive X-ray Analysis (EDAX). The functional groups present in the nanocomposite were identified by Fourier Transform Infra-Red (FTIR) spectroscopy and Fourier Transform Raman (FT Raman) spectroscopy. The optical properties were identified by Ultraviolet-Visible spectroscopy and Photoluminescence spectroscopy. Zeta potential measurements were done to determine the surface charge of the sample. The antibacterial activity was identified for three gram-positive bacteria and seven gram-negative bacteria.

3.1 X-Ray Diffraction

Figure 2 shows the X-Ray diffraction spectra of Nano Silicon dioxide (SiO_2) combined with Zinc oxide (ZnO) prepared by hydrothermal method. (Avg. Crystallite size = 5.18 nm). CuKα radiation was used with wavelength 1.5406 Å [19]. Peaks obtained were in good agreement with JCPDS card no. 00-024-1468 known as Zinc silicate. The crystal system is orthorhombic [20] with Pcab space group. Sharp peaks obtained shows the crystalline nature of zinc oxide with nano silica. The peak at around 21° is a characteristic peak of nano-silica, and the remaining peaks indicate the presence of "zinc silicate". Diffraction peaks at 21°, 24°, 32° and 58° corresponds with miller indices (100), (220), (040) and (522) respectively [21].

The crystallite size was found from Debye-Scherrer's equation:

$$D = \frac{k\lambda}{\beta \cos \theta}$$

Where,

k – constant (0.94)

λ – wavelength of X-ray (1.5406 Å)

β – full width half maxima (FWHM)

θ – angle of diffraction [22]

The crystallite size for different peak positions 21°, 24°, 32° and 58° are 34.2 nm, 32.8 nm, 31.4 nm, 33.6 nm respectively. The average crystallite size was found to be 33 nm.

Figure 2: XRD Pattern Of Silica With Zinc Oxide

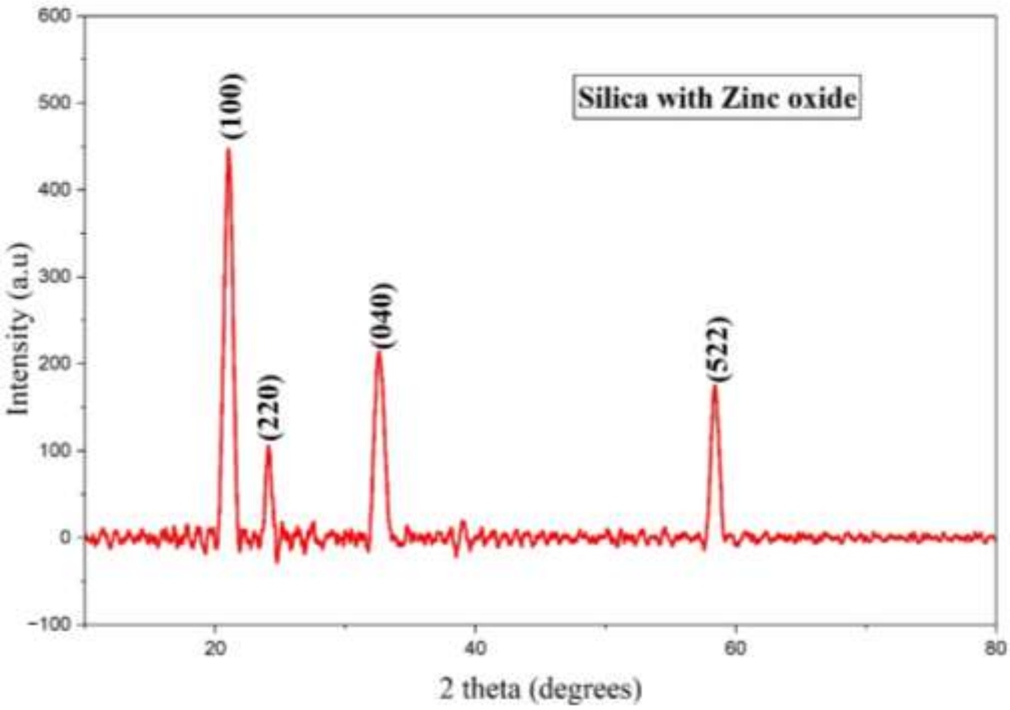

Figure 3 shows the stress strain plot of zinc oxide with nano silica. The micro-strain was calculated from the slope of Williamson-Hall plot shown above by using the formula:

$$\varepsilon = \frac{\beta}{4\tan\theta}$$

Where,
ε – micro-strain in radians/ ratio of peak width to peak position
β – line broadening at FWHM in radians
θ – Bragg's angle in degrees, half of 2θ
The dislocation density was calculated using the formula [23]:

$$\delta = \frac{1}{t^2}$$

Where,
t – crystallite size in nm
The value of micro-strain and dislocation density were found to be 0.0128×10^{-3} and 0.0091×10^{-3} respectively.

Figure 3: Micro-Strain Plot Of Silica With Zinc Oxide

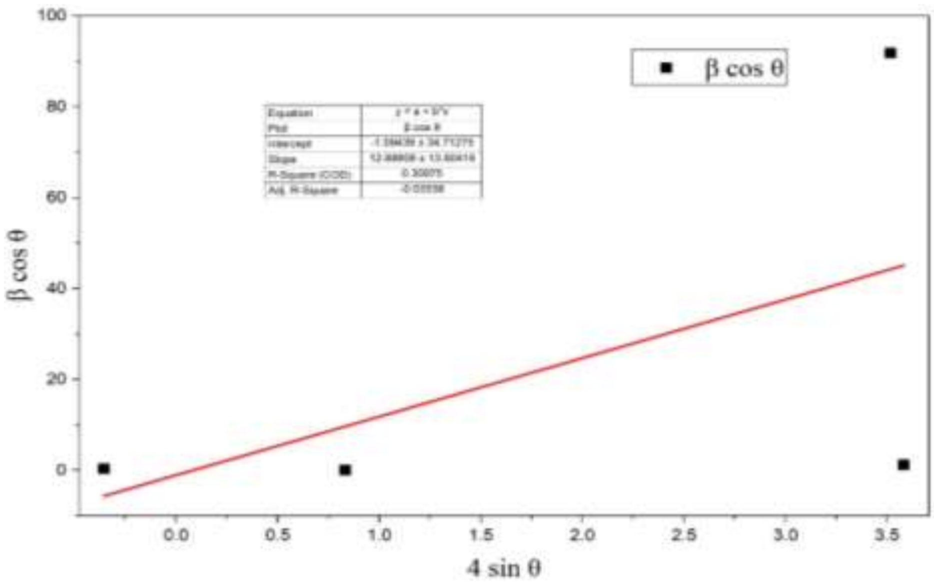

3.2 Field Emission Scanning Electron Microscopy (FESEM) with Energy Dispersive X-ray Analysis (EDAX):

Figures 4a and 4b show the Field Emission Scanning Electron Microscopy (FESEM) images of Zinc oxide with Nano Silica at 1 µ-m and 5 µ-m magnifications respectively. The surface morphology of the sample prepared by hydrothermal method was studied under Scanning Electron Microscope [24]. Powder sample was dispersed in ethanol and ultra-sonicated, then coated on an aluminum foil of dimension 1×1 cm and dried before analysis Images show the irregular agglomerated spherical morphology [25] of the coated samples [26]. The quantity of silica precursor has an effect on the morphology of the material [27]. The average diameter of particles calculated using ImageJ Software and Origin Software was found to be 7.38 nm. The histogram plot [28] obtained for finding the diameter of Zinc oxide with Nano Silica nanocomposite is shown in figure 5.

Figure 4a: FESEM Image Of Silica With Zinc Oxide At 1 M-M Magnification

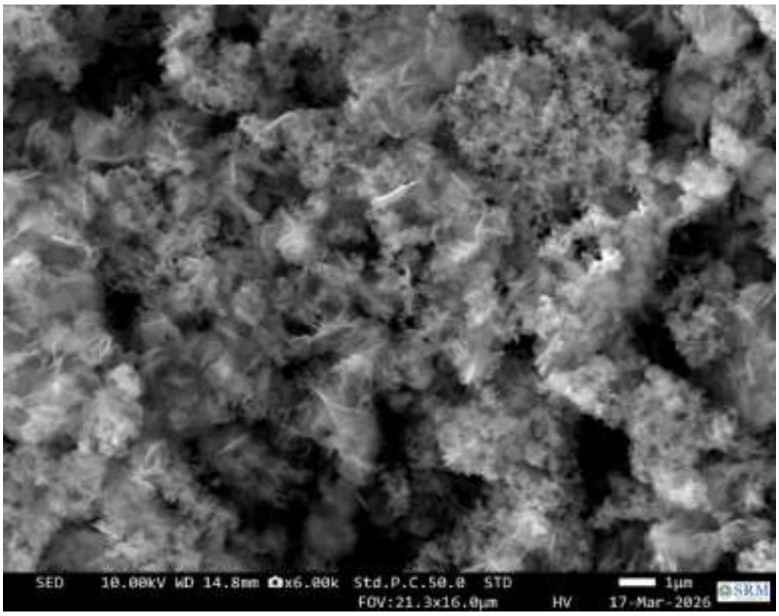

Figure 4b: FESEM Image Of Silica With Zinc Oxide At 5 M-M Magnification

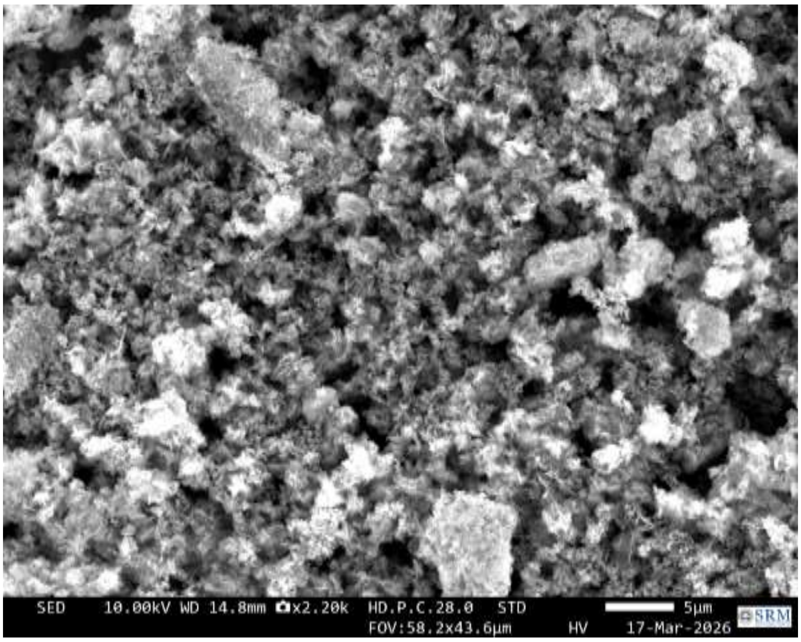

Figure 5: Histogram Plot To Find Diameter Of Silica With Zinc Oxide

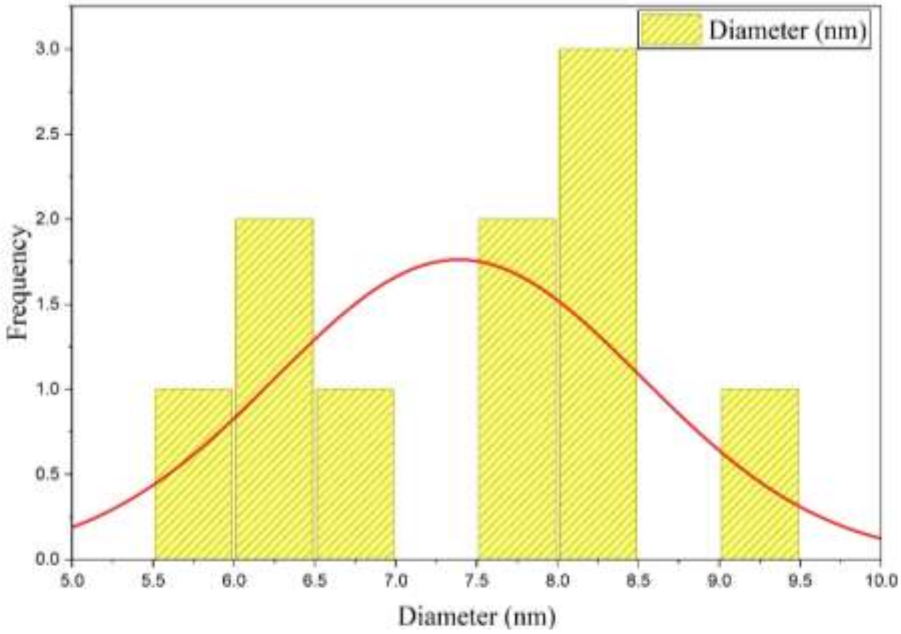

3.2a Energy Dispersive X-Ray Analysis (EDAX):

Figure 6 shows the Energy Dispersive X-ray Spectrum of Zinc oxide with Nano-Silica with Energy in kilo electron volt (keV) on the horizontal axis and Count per second in electron volt (eV) on the vertical axis. To confirm the formation of silica and zinc oxide, EDAX analysis was performed. Spectra clearly show the peaks of silicon (Si), zinc (Zn) and oxygen (O) [26]. In addition to it, carbon (C) is present as impurity [28]. The atomic concentration of Si, Zn and O were 14.91%, 4.69% and 45.14% respectively and the mass concentration of Si, Zn and O were 23.77%, 17.4% and 40.99% respectively . Details of Silica with Zinc oxide nanocomposite EDAX spectra values are listed in the table 1.

Table 1: Elemental Analysis Of Silica With Zinc Oxide From EDAX Spectra

Element	Atomic number	Net counts	Mass Concentration /%	Norm. mass concentration /%	Norm. atomic concentration /%	3σ uncertainty /mass%
O	8	25122	40.99	38.60	45.14	1.93
C	6	6971	24.04	22.64	35.27	1.66
Si	14	36265	23.77	22.38	14.91	3.19
Zn	30	17467	17.40	16.38	4.69	3.56
		Sum	**106.20**	**100.00**	**100.00**	

Figure 6: Elemental Composition Of Silica With Zinc Oxide

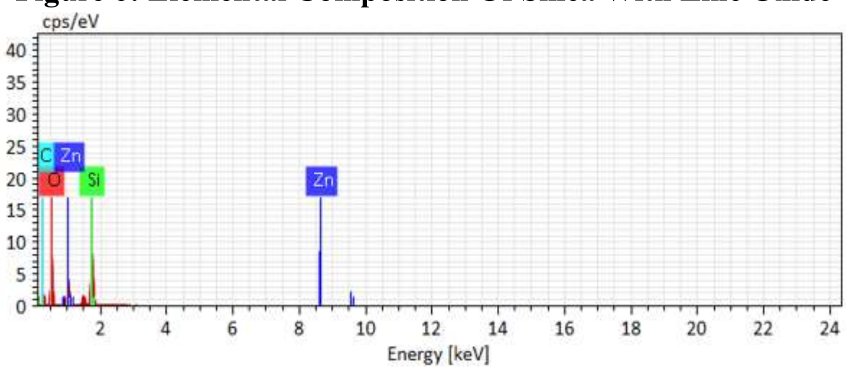

3.3 High-Resolution Transmission Electron Microscopy (HRTEM) with Selected Area Electron Diffraction (SAED) analysis

Highly magnified internal microstructures of Zinc oxide with Nano-Silica at magnification 200 nm and 500 nm, prepared by hydrothermal method using TEOS precursor and CTAB as surfactant are shown in figures 7a and 7b. Ethanol was used to suspend the particles and the solution was dropped in coated grids, dried and viewed under microscope with accelerating voltage 80 kV. Transmission Electron Microscopy images at high resolution indicate the formation of irregular spherical nanoparticles [29] of Zinc oxide with Silica. The average particle size was found using ImageJ Software as 61.5 nm. Higher particle size is due to the agglomeration of spherical nanostructures [30], from the images, cluster-like morphology of particles is clearly seen.

Figure 7a: HRTEM Image Of Silica With Zinc Oxide At 200 Nm Magnification

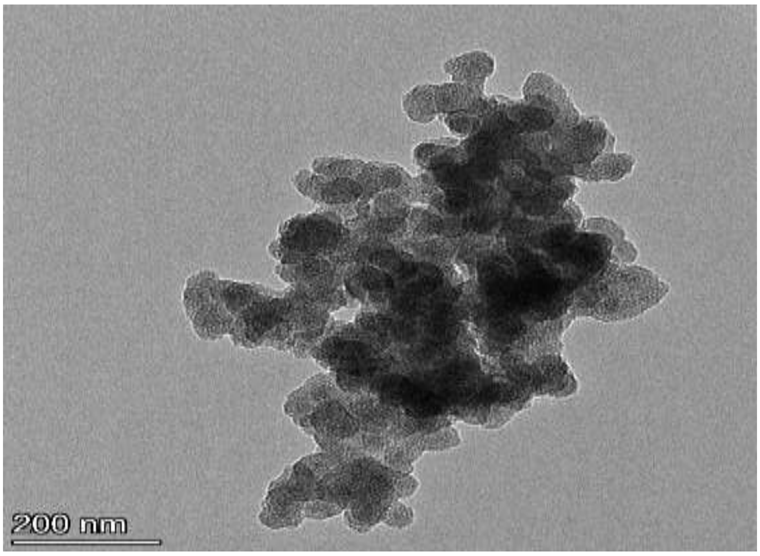

Figure 7b: HRTEM Image Of Silica With Zinc Oxide At 500 Nm Magnification

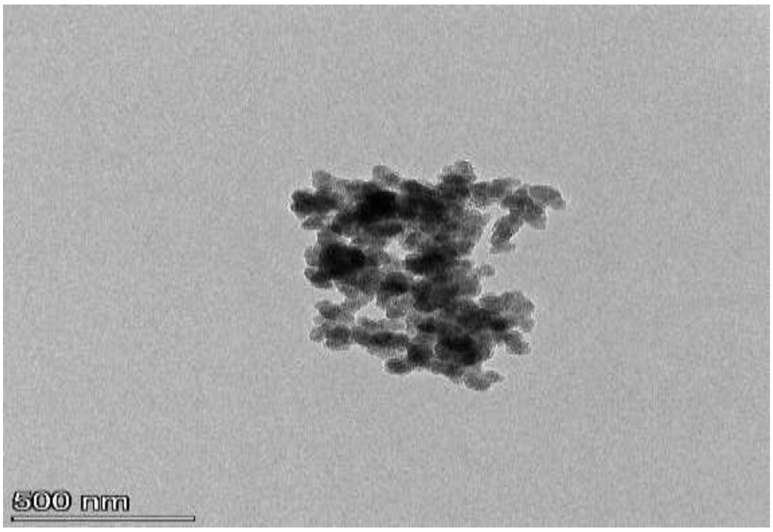

3.3a Selected Area Electron Diffraction (SAED)

To display the accurate local crystal structure of Zinc oxide with Nano-Silica, SAED analysis was done at 5 nm^{-1} magnification [31]. Pattern shows diffuse halo concentric rings with few spot-like structures which indicate that the internal structure of nanocomposite is crystalline embedded in an amorphous material

[32]. The d-spacing values in Å were found to be 6.74, 3.20, 1.88 and 0.95 which corresponds to miller indices (020), (220), (123) and (321) respectively. These are indexed as shown in figure 8. By comparing the d-spacing values obtained from XRD and SAED, rings that exist at (020) and (220) strongly indicate the presence of Zinc oxide with Silica nanocomposite.

Figure 8: SAED Pattern Of Silica With Zinc Oxide

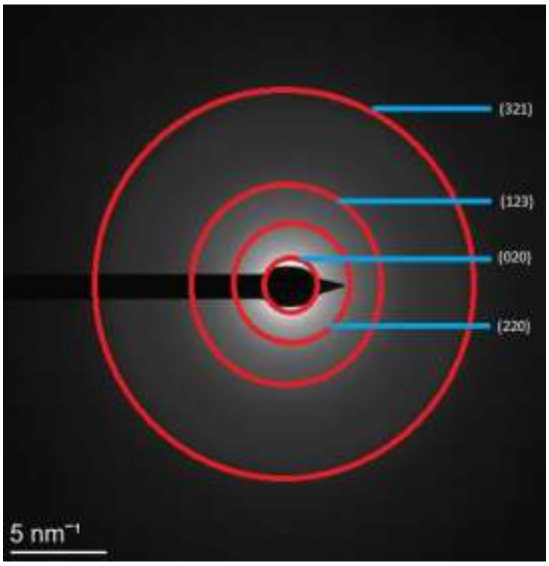

3.4 Ultraviolet-Visible (UV-Vis) Spectroscopy

Figure 9 shows the UV spectrum and Tauc's plot of Zinc oxide with Nano-silica. Optical absorbance spectra [33] of Zinc oxide with Nano-silica were recorded in the wavelength region from 200 to 800 nm. From the absorbance spectra, optical band gap energy of Zinc oxide with Nano-silica were calculated by Tauc's relation:

$$\alpha h\gamma = A(h\gamma - E_g)^n$$

Where $h\gamma$ – incident photon energy

α – absorption coefficient

A – constant

E_g – band gap of the material

n – depends on the type of the transition for direct band gap material [34]

Optical band gap was calculated by extrapolating a line on the linear part of the curve intercepting the X-axis ($h\gamma$ in eV) [35]. Energy band gap of materials is calculated using the Tauc plot method [36]. The observed band gap energy from the Tauc's plot [37] is found to be 5.6 eV.

Figure 9: UV Spectrum And Tauc's Plot Of Silica With Zinc Oxide

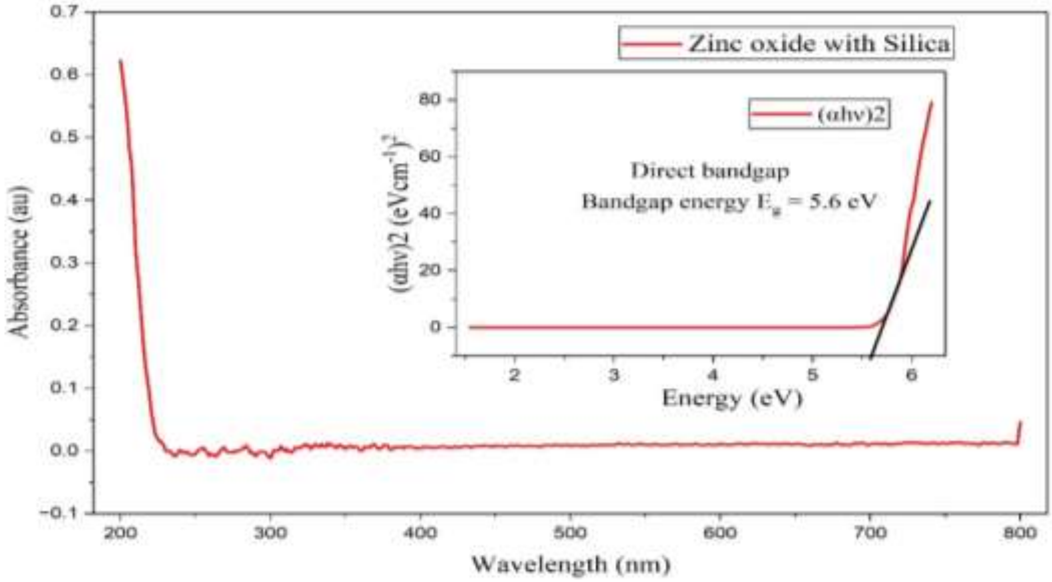

3.5 Photoluminescence (PL) Spectroscopy

Figure 10 shows the Photoluminescence emission spectrum of Zinc oxide with Nano-Silica. The intensity was measured at room temperature between the wavelength range 250 nm and 700 nm. To validate the transfer of charges which leads to emission, photoluminescence was performed at a particular wavelength range [38]. The PL emission spectrum [39] was recorded with 330 nm as the excitation wavelength for Zinc oxide nanostructures using Photoluminescence spectrophotometer. The broad peak in the UV region is related to the recombination of excited electron in the conduction band and a hole from the valence band in band-gap region. The emission peaks in the visible region are due to the oxygen and interstitial defects in Zinc oxide nanostructures. Zinc oxide is potential material for higher photoluminescence efficiency [40]. Emission intensity increases with a rise in zinc oxide content in the nanocomposite [41].

Figure 10: Photoluminescence Of Silica With Zinc Oxide

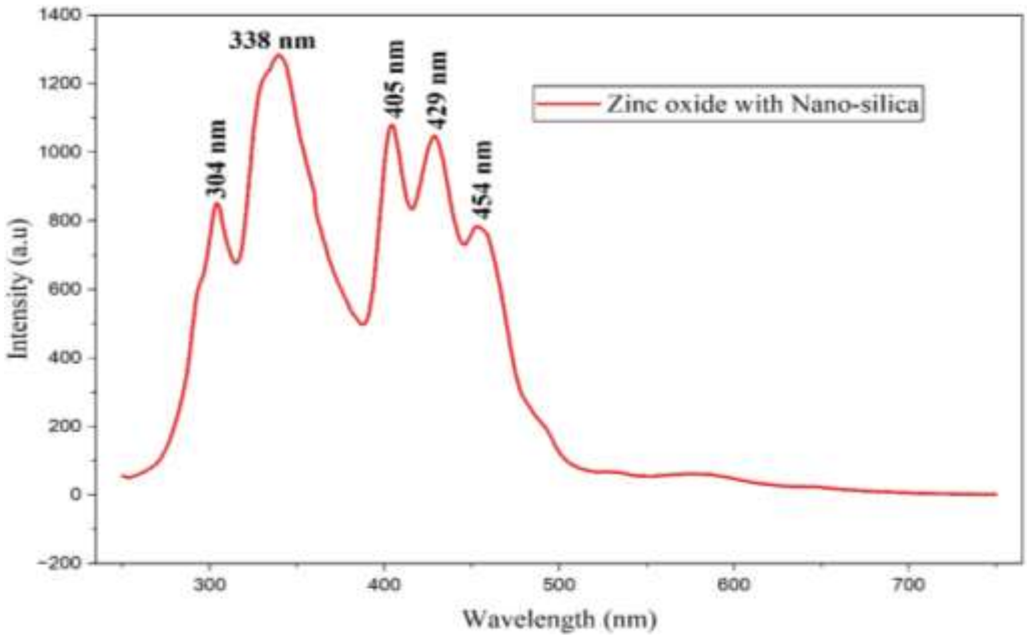

3.6 Fourier Transform Infrared Spectroscopy (FTIR)

Figure 11 shows the Fourier Transform Infrared (FTIR) Spectrum of zinc oxide with nano-silica. The functional groups were identified within the wavenumber range from 4000 cm^{-1} to 400 cm^{-1} using Shimadzu IR Tracer-100 FTIR spectrometer. The graph is plotted with wavenumber (cm^{-1}) in the X-axis and transmittance or absorbance (%) in the Y-axis [42]. The main peak at 449 cm^{-1} corresponds to inorganic metal-oxygen M-O stretching group. The different peaks at 2924 cm^{-1}, 1569 cm^{-1} and 1053 cm^{-1} corresponds to O-H stretching, C=C stretching and C-O stretching vibrations respectively. The peaks at 1423 cm^{-1} and 794 cm^{-1} corresponds to O-H bending and C=C bending vibrations respectively. The two peaks at around 1569 cm^{-1} and 1423 cm^{-1} confirms the presence of zinc oxide ions [43]. The peak at around 1053 cm^{-1} indicates the presence of silica (Si-O-Si) bond and the peak at around 449 cm^{-1} confirms the bond formed by zinc oxide [44].

Figure 11: FTIR Spectrum Of Silica With Zinc Oxide

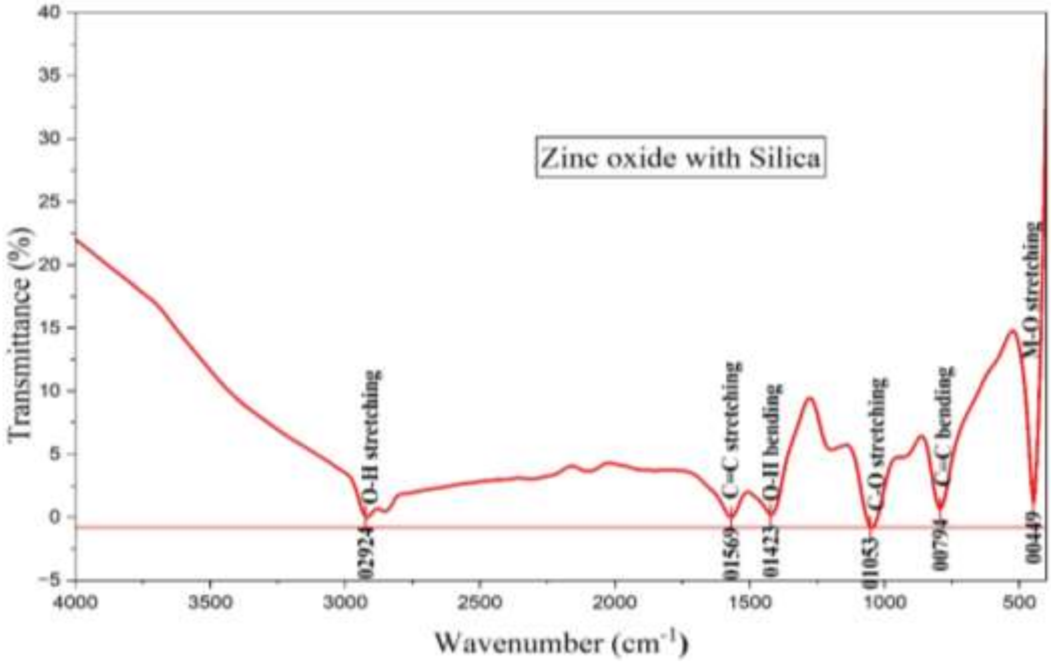

3.7 Fourier Transform Raman Spectroscopy (FT Raman)

Figure 12 shows the Fourier Transform Raman Spectroscopy (FT Raman) graph of Zinc oxide with Nano-Silica. Raman spectrum of silica with zinc oxide nanocomposite plotted against Raman shift and Intensity is shown [45]. To evaluate the structural properties and phase composition of the material, Raman spectroscopy analysis was done [46]. The peaks at 458 cm^{-1} and 467 cm^{-1} correspond to metal-oxygen inorganic class of compounds with M-O stretching group. The peak at 507 cm^{-1} corresponds to halo compounds class with C-I stretching group. The peak at 529 cm^{-1} corresponds to low diamond band with sp^3 carbon. The peaks at 557 cm^{-1}, 566 cm^{-1} and 594 cm^{-1} corresponds to a class of halo compounds with C-Br stretching group. The band at around 467 cm^{-1} indicates the presence of silica [47].

Figure 12: FT Raman Spectrum Of Silica With Zinc Oxide

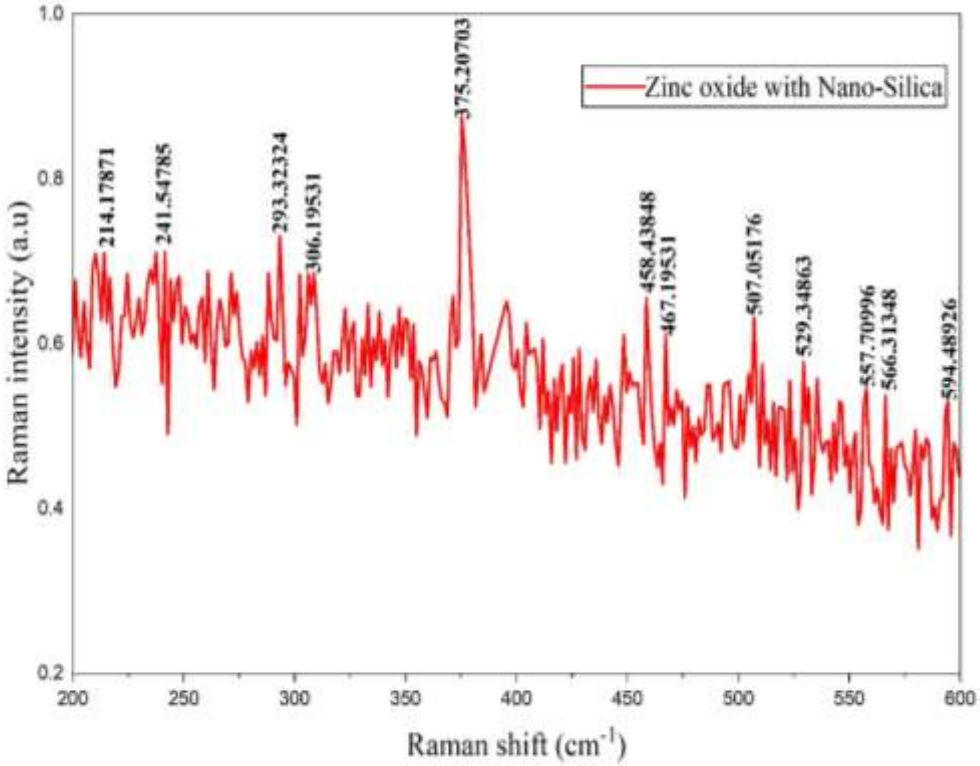

3.8 Zeta potential

Figure 13 shows the zeta potential graph of Zinc oxide with Nano-silica. Zeta potential measurements were taken from Horiba Scientific SF-100 to determine the surface charge of the sample. The temperature, pH and concentration of the material have an effect on the zeta potential values [48]. The surface charge was analyzed using a Temperature of the Holder 25°C, Dispersion Medium Viscosity 0.894 mPa-s, Conductivity 0.104 mS/cm and Electrode Voltage 3.4V. Analysis was taken after powder sample was dispersed in distilled water and filtered using syringe filter. Zeta potential analysis was done using a Zeta-sizer, Malvern Panalytical Ltd [49]. The charge of the sample's surface was found to be negative with a Mean Zeta Potential value -1.6 mV and Mean Electrophoretic Mobility -0.12 × 10^{-4} cm^2/Vs

Figure 13: Zeta Potential Graph Of Silica With Zinc Oxide

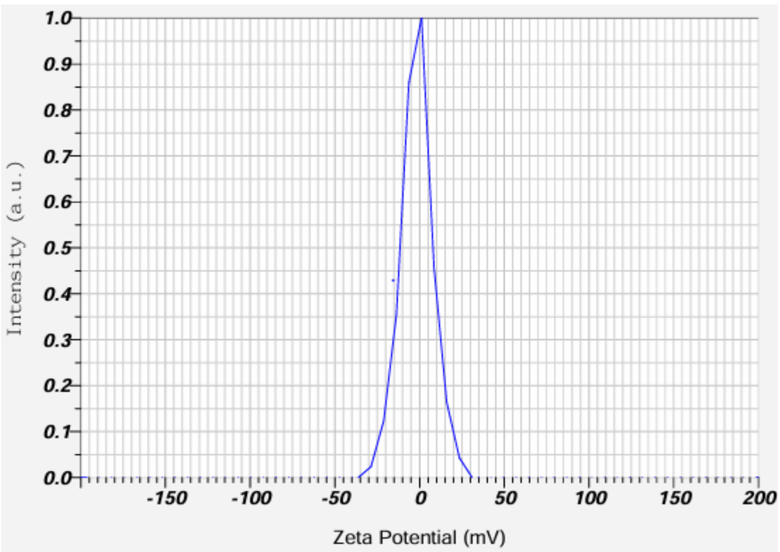

4. Antibacterial Properties

Bacteria show resistance to conventional antibiotics. As a result, it is crucial to find alternative drugs to inhibit bacterial growth. Metal and metal oxides play a vital role in destroying bacterial growth of several gram-positive and gram-negative bacteria. Zinc oxide is a promising material which has high antibacterial efficacy [50]. It has high stability, biocompatibility and used in pharmaceutical industry owing to its significant bacterial inhibitory potential [51].

4.1 Test culture

The bacterial cultures used for testing were obtained from the Department of Microbiology at Ethiraj College, Chennai, India. The *Escherichia coli* (ATCC 25922) and *Salmonella typhimurium* strains (ATCC 14028) were procured from Hi-Media Laboratories.

4.2 Tested organisms

Three Gram-positive bacteria such as *Staphylococcus aureus, Enterococcus* species, and *Streptococcus pyogenes,* were used. Seven Gram-negative bacteria such as *Escherichia coli, Escherichia coli* (ATCC 25922) strain, *Klebsiella pneumoniae*, *Salmonella* species, *Pseudomonas aeruginosa, Proteus* species, and *Salmonella typhimurium* (ATCC 14028) strain, were used in the present study.

4.3 Test sample

Zinc oxide with Nano-Silica (Sample code: CS6)

4.4 Inoculum preparation

The bacterial cultures were grown in Muller-Hinton Broth (MHB) at 37 °C for 24h incubation. After incubation, the 24-hour-old culture is ready for an antibacterial susceptibility test. Before starting the test, the inoculum tube was adjusted visually by either adding bacterial colonies if the concentration is too light or by adding sterile normal saline solution if the concentration is too thick. This was done to match the already prepared 0.5 McFarland standard, which is assumed to contain a bacterial concentration of 1×10^8 colony-forming unit (CFU)/mL [52]

4.5 Disc diffusion method

Antibacterial activity was carried out using the disc-diffusion method. Petri plates were prepared with 20 ml of sterile Mueller-Hinton Agar (MHA) and made to solidify. About 100µl of bacterial suspension containing 10^8 CFU/ml bacteria were swabbed on the top of the solidified media and allowed to dry for 10 min. The test was conducted at 1 mg/disc concentration each and 25µl/disc for the test sample Zinc oxide with Nano-Silica (CS6). The loaded discs were placed on the surface of the agar medium and left for 30 min at room temperature for compounds to diffuse into the medium. Ciprofloxacin (5µg /disc) was used as a positive control (PC) and DMSO - Dimethyl Sulfoxide (25µl/disc) was used as a negative control (NC). The plates were incubated for 24 h at 37°C. After the incubation period, the zone of inhibition (the area around the discs where the bacterial growth was inhibited) was recorded in millimetres [53].

4.6 Results

The results of antibacterial activity revealed that the samples at 1 mg/disc were tested against gram-positive and gram-negative pathogenic microorganisms.

Zinc oxide with Nano-Silica showed antibacterial activity against gram-positive bacteria such as *Staphylococcus aureus* (12mm) [54], *Streptococcus pyogenes* (10mm), *Enterococcus* species (12mm), and gram-negative bacteria such as *Escherichia coli* (09mm), *Pseudomonas aeruginosa* (11mm) [55], *Proteus* species (10mm), *Salmonella* species (11mm), *Klebsiella pneumonia* (11mm), *Escherichia coli* - 25922 (11mm) [56], and *Salmonella typhimurium* - 14028 (11mm) at 1 mg/disc.

Ciprofloxacin 5µg/disc was used as a standard control (PC), and Dimethyl Sulfoxide (DMSO) 25µl/disc was used as the negative control (NC).
Figures 14a to 14j show the antibacterial activity, the zone of inhibition of ten bacterial species by Zinc oxide with Silica nanocomposite.

Figures 14a – 14j: Antibacterial Activity Of Silica With Zinc Oxide Nanocomposite On Ten Different Bacteria

Staphylococcus aureus

Streptococcus pyogenes

Enterococcus species

Escherichia coli

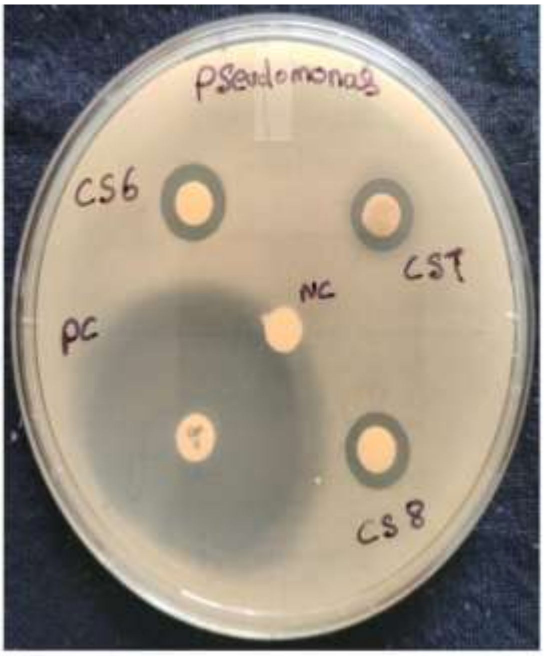

Pseudomonas aeruginosa

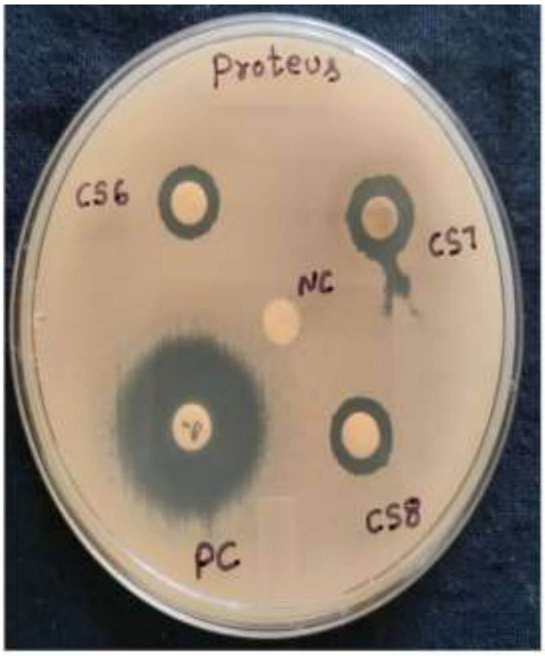

Proteus species

Salmonella species

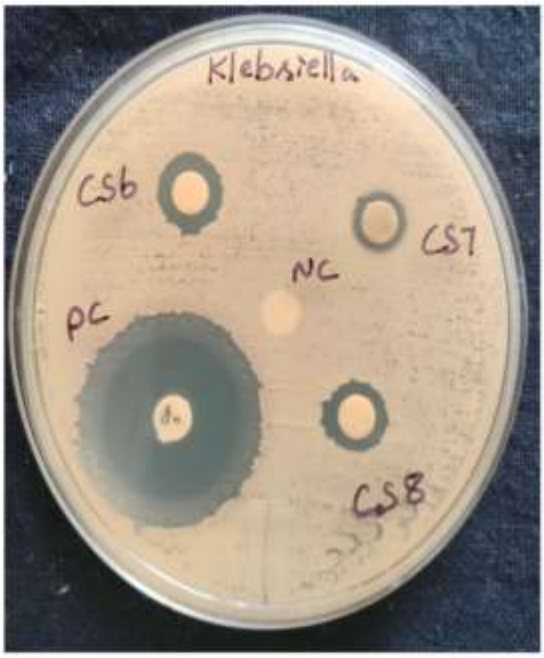

Klebsiella pneumoniae

Salmonella typhimurium - 14028

Escherichia coli - 25922

5. Conclusion

Thus, Tetraethyl orthosilicate (TEOS) was used as precursor for Nano-Silica, Cetyl Trimethyl Ammonium Bromide (CTAB) was used as surfactant for morphology control of the sample, Zinc acetate dihydrate was used as precursor for Zinc oxide nanoparticles. Silica with Zinc oxide nanocomposite was synthesized by following the “Hydrothermal” method of synthesis. The material was subjected to high temperature and cooled rapidly by deep freezing followed by freeze-drying the sample. White powder of Silica with Zinc oxide nanocomposite was obtained.

Then, the morphological and structural properties were identified by X-Ray Diffraction (XRD), Field Emission Scanning Electron Microscopy (FESEM), High-Resolution Transmission Electron Microscopy (HRTEM) and Selected Area Electron Diffraction (SAED). The elemental analysis and chemical composition of the sample was identified by Energy Dispersive X-ray Analysis (EDAX). The functional groups present in the sample were determined by Fourier Transform Infrared Spectroscopy (FTIR) and Fourier Transform Raman (FT Raman) Spectroscopy. The optical band gap was identified from Ultraviolet-Visible (UV-Vis) Spectroscopy. The surface charge of the nanocomposite was found using Zeta potential.

Finally, the antibacterial properties of zinc oxide were found from “Disc-diffusion method”. The zone of inhibition of three gram-positive bacteria and seven gram-negative bacteria were identified. Thus, silica with zinc oxide nanocomposite was proved to be an efficient nanocomposite against pathogenic bacteria.

6. Acknowledgement

Dr. N.S. Nirmala Jothi, who is the second author to this Research article is the guide, the entire work was proceeded under her guidance and supervision. The experimental work was carried out in Centre for Excellence in Materials and Advanced Technologies (CeMAT), SRM Institute of Science and Technology, Kattankulathur. All the basic characterizations were taken from Nanotechnology Research Centre (NRC) and School of Bioengineering, SRM University.

8. References:

1. Nikolova MP, Chavali MS. Metal oxide nanoparticles as biomedical materials. Biomimetics 2020;5.

https://doi.org/10.3390/BIOMIMETICS5020027.
2. Murthy S, Effiong P, Fei CC. Metal oxide nanoparticles in biomedical applications. Metal Oxide Powder Technologies: Fundamentals, Processing Methods and Applications, Elsevier; 2020, p. 233–51. https://doi.org/10.1016/B978-0-12-817505-7.00011-7.
3. Makvandi P, Wang C yu, Zare EN, Borzacchiello A, Niu L na, Tay FR. Metal-Based Nanomaterials in Biomedical Applications: Antimicrobial Activity and Cytotoxicity Aspects. Adv Funct Mater 2020;30. https://doi.org/10.1002/adfm.201910021.
4. Varshney S, Nigam A, Pawar SJ, Mishra N. An overview on biomedical applications of versatile silica nanoparticles, synthesized via several chemical and biological routes: A review. Phosphorus Sulfur Silicon Relat Elem 2022;197:72–88. https://doi.org/10.1080/10426507.2021.2017434.
5. Huang Y, Li P, Zhao R, Zhao L, Liu J, Peng S, et al. Silica nanoparticles: Biomedical applications and toxicity. Biomedicine and Pharmacotherapy 2022;151. https://doi.org/10.1016/j.biopha.2022.113053.
6. Selvarajan V, Obuobi S, Ee PLR. Silica Nanoparticles—A Versatile Tool for the Treatment of Bacterial Infections. Front Chem 2020;8. https://doi.org/10.3389/fchem.2020.00602.
7. Alavi M, Thomas S, Sreedharan M. Micro Nano Bio Aspects Modification of silica nanoparticles for antibacterial activities: mechanism of action. Micro Nano Bio Aspects 2022;2022:49–58. https://doi.org/10.22034/mnba.2022.153448.
8. Fu T, Duan B, Sun P, Ma W, Wang T, Wang T, et al. Innovative applications of silicon dioxide nanoparticles for targeted liver cancer treatment. Front Bioeng Biotechnol 2025;13. https://doi.org/10.3389/fbioe.2025.1595772.
9. Mandal AK, Katuwal S, Tettey F, Gupta A, Bhattarai S, Jaisi S, et al. Current Research on Zinc Oxide Nanoparticles: Synthesis, Characterization, and Biomedical Applications. Nanomaterials 2022;12. https://doi.org/10.3390/nano12173066.
10. Islam F, Shohag S, Uddin MJ, Islam MR, Nafady MH, Akter A, et al. Exploring the Journey of Zinc Oxide Nanoparticles (ZnO-NPs) toward Biomedical Applications. Materials 2022;15. https://doi.org/10.3390/ma15062160.
11. Asif N, Amir M, Fatma T. Recent advances in the synthesis, characterization and biomedical applications of zinc oxide nanoparticles. Bioprocess Biosyst Eng 2023;46:1377–98. https://doi.org/10.1007/s00449-023-02886-1.
12. Ramesh P, Saravanan K, Manogar P, Johnson J, Vinoth E, Mayakannan M. Green synthesis and characterization of biocompatible zinc oxide nanoparticles and evaluation of its antibacterial potential. Sens Biosensing Res 2021;31. https://doi.org/10.1016/j.sbsr.2021.100399.
13. Mendes CR, Dilarri G, Forsan CF, Sapata V de MR, Lopes PRM, de Moraes PB, et al. Antibacterial action and target mechanisms of zinc oxide nanoparticles against bacterial pathogens. Sci Rep 2022;12. https://doi.org/10.1038/s41598-022-06657-y.
14. Jin S-E, Jin H-E. Antimicrobial Activity of Zinc Oxide Nano/Microparticles and Their Combinations against Pathogenic Microorganisms for Biomedical Applications: From Physicochemical Characteristics to Pharmacological Aspects 2021. https://doi.org/10.3390/nano110.
15. Alhujaily M, Albukhaty S, Yusuf M, Mohammed MKA, Sulaiman GM, Al-Karagoly H, et al. Recent Advances in Plant-Mediated Zinc Oxide Nanoparticles with Their Significant Biomedical Properties. Bioengineering 2022;9. https://doi.org/10.3390/bioengineering9100541.
16. Li Y, Liao C, Tjong SC. Recent advances in zinc oxide nanostructures with antimicrobial activities. Int J Mol Sci 2020;21:1–70. https://doi.org/10.3390/ijms21228836.

17. Halbus AF, Horozov TS, Paunov VN. Surface-Modified Zinc Oxide Nanoparticles for Antialgal and Antiyeast Applications. ACS Appl Nano Mater 2020;3:440–51. https://doi.org/10.1021/acsanm.9b02045.
18. Panigrahi G, Medhi H, Wasnik K, Patra S, Gupta P, Pareek D, et al. Hollow mesoporous SiO2–ZnO nanocapsules and effective in vitro delivery of anticancer drugs against different cancers with low doses of drugs. Mater Chem Phys 2022;287. https://doi.org/10.1016/j.matchemphys.2022.126287.
19. Channe SS, Singh R, Kulkarni SG. Effect of metal oxide nanoparticles on thermal behavior of polyvinyl alcohol. Polymer Bulletin 2024;81:3403–38. https://doi.org/10.1007/s00289-023-04858-7.
20. Beglaryan H, Isahakyan A, Zulumyan N, Melikyan S, Terzyan A. A study of zinc silicate phases produced via a simplified method. J Therm Anal Calorim 2023;148:3249–62. https://doi.org/10.1007/s10973-023-11949-0.
21. Ali A, Saeed S, Hussain R, Afzal G, Siddique AB, Parveen G, et al. Synthesis and Characterization of Silica, Silver-Silica, and Zinc Oxide-Silica Nanoparticles for Evaluation of Blood Biochemistry, Oxidative Stress, and Hepatotoxicity in Albino Rats. ACS Omega 2023;8:20900–11. https://doi.org/10.1021/acsomega.3c01674.
22. Al-Selwey WA, Alsadon AA, Ibrahim AA, Labis JP, Seleiman MF. Effects of Zinc Oxide and Silicon Dioxide Nanoparticles on Physiological, Yield, and Water Use Efficiency Traits of Potato Grown under Water Deficit. Plants 2023;12. https://doi.org/10.3390/plants12010218.
23. Hussein AS, Al Jasmi FSO, Jawad MH, Fahem MQ. Fabrication and Characterisation of Zinc Oxide (ZnO) Grown on Porous Silicon (PSi) Substrate Using Different Techniques for Glucose Biosensor. Silicon 2025. https://doi.org/10.1007/s12633-025-03553-8.
24. Hassan SM ul, Anis T, Khurshid A, Shahzad F, Iqbal Z, Ali Z, et al. Facile synthesis of multifunctional m-SiO2@ZnO nanocomposite employing biocompatible polymers for potential theranostic applications. Micro Nano Lett 2021;16:149–56. https://doi.org/10.1049/mna2.12028.
25. Safavinia L, Akhgar MR, Tahamipour B, Ahmadi SA. Green synthesis of highly dispersed zinc oxide nanoparticles supported on silica gel matrix by daphne oleoides extract and their antibacterial activity. Iran J Biotechnol 2021;19:86–95. https://doi.org/10.30498/IJB.2021.2598.
26. Bhushan D, Gupta R. Biofabrication and Characterization of Silica-coated Zinc Oxide Nanocomposite: A Sustainable Approach in Remediation of Cr(VI) Contaminated Wastewater. Water Air Soil Pollut 2024;235. https://doi.org/10.1007/s11270-024-07182-6.
27. Qin X, Cai H, Wang F, Xu Y. Hydrothermal Synthesis of Zinc Silicate Nanomaterials for Organic Dyes Removal from Aqueous Solutions. Silicon 2024;16:6031–9. https://doi.org/10.1007/s12633-024-03135-0.
28. Shaba EY, Tijani JO, Jacob JO, Suleiman MAT. Effect of mixing ratios of SiO2 nanoparticles synthesized from metakaolin on the physicochemical properties of ZnO/SiO2 nanocomposites. Nano-Structures and Nano-Objects 2023;35. https://doi.org/10.1016/j.nanoso.2023.101003.
29. Haroun SA, Elnaggar ME, Zein DM, Gad RI. Insecticidal efficiency and safety of zinc oxide and hydrophilic silica nanoparticles against some stored seed insects. J Plant Prot Res 2020;60:77–85. https://doi.org/10.24425/jppr.2020.132211.
30. Qomariyah L, Hirano T, Putra NR, Suprapto S, Ajiz HA, Fauziyah M. Innovative surfactant-free synthesis of core-shell SiO2/ZnO particles: rapid ultrasonication and photocatalytic inhibition. RSC Adv 2024;14:12665–75. https://doi.org/10.1039/d4ra01309c.

31. Durgude SA, Ram S, Kumar R, Singh SV, Singh V, Durgude AG, et al. Synthesis of Mesoporous Silica and Graphene-Based FeO and ZnO Nanocomposites for Nutritional Biofortification and Sustained the Productivity of Rice (Oryza sativa L.). J Nanomater 2022;2022. https://doi.org/10.1155/2022/5120307.
32. Easwaran G, Vijayan M, Sivakumar K, Bhuvaneswari K, Palanisamy G. Zinc Oxide Nanoparticles Decorated on Arundo donax L. Plant Leaves Derived Silica Nanosheets for Enriched Catalytic Degradation of Organic Dye Under UV-Visible Light Irradiation. Silicon 2023;15:1725–37. https://doi.org/10.1007/s12633-022-02122-7.
33. Jia Z, Hong R. Anticorrosive and photocatalytic properties research of epoxy-silica organic–inorganic coating. Colloids Surf A Physicochem Eng Asp 2021;622. https://doi.org/10.1016/j.colsurfa.2021.126647.
34. Mursyalaat V, Variani VI, Arsyad WOS, Firihu MZ. The development of program for calculating the band gap energy of semiconductor material based on UV-Vis spectrum using delphi 7.0. J. Phys. Conf. Ser., vol. 2498, Institute of Physics; 2023. https://doi.org/10.1088/1742-6596/2498/1/012042.
35. Jubu PR, Obaseki OS, Yam FK, Stephen SM, Avaa AA, McAsule AA, et al. Influence of the secondary absorption and the vertical axis scale of the Tauc's plot on optical bandgap energy. Journal of Optics (India) 2023;52:1426–35. https://doi.org/10.1007/s12596-022-00961-6.
36. Johannes AZ, Pingak RK, Bukit M. Tauc Plot Software: Calculating energy gap values of organic materials based on Ultraviolet-Visible absorbance spectrum. IOP Conf. Ser. Mater. Sci. Eng., vol. 823, Institute of Physics Publishing; 2020. https://doi.org/10.1088/1757-899X/823/1/012030.
37. Abdel Messih MF, Shalan AE, Ahmed MA, Sanad MF. Zinc oxide-supported silica gel (ZnO–SiO2) as a sun light-driven photocatalyst. Journal of Materials Science: Materials in Electronics 2024;35. https://doi.org/10.1007/s10854-024-12617-1.
38. Mondal US, Das S, Somu P, Paul S. Silica sand–supported nano zinc oxide–graphene oxide composite induced rapid photocatalytic decolorization of azo dyes under sunlight and improved antimicrobial activity. Environmental Science and Pollution Research 2023;30:17226–44. https://doi.org/10.1007/s11356-022-23248-6.
39. Parkhomenko I, Vlasukova L, Komarov F, Makhavikou M, Milchanin O, Wendler E, et al. Luminescence of ZnO nanocrystals in silica synthesized by dual (Zn, O) implantation and thermal annealing. J Phys D Appl Phys 2021;54. https://doi.org/10.1088/1361-6463/abf0ec.
40. Liu ZY, Shen CL, Lou Q, Zhao WB, Wei JY, Liu KK, et al. Efficient chemiluminescent ZnO nanoparticles for cellular imaging. J Lumin 2020;221. https://doi.org/10.1016/j.jlumin.2020.117111.
41. Wahab SAA, Matori KA, Aziz SHA, Zaid MHM, Kechik MMA, Azman AZK, et al. Effect of ZnO on the phase transformation and optical properties of silicate glass frits using rice husk ash as a SiO2 source. Journal of Materials Research and Technology 2020;9:11013–21. https://doi.org/10.1016/j.jmrt.2020.08.005.
42. Mansour AM, Abou Hammad AB, Bakr AM, El Nahrawy AM. Silica Zinc Titanate Wide Bandgap Semiconductor Nanocrystallites: Synthesis and Characterization n.d. https://doi.org/10.1007/s12633-022-01886-2/Published.
43. Buşilă M, Tăbăcaru A, Muşsat V, Vasile BŞ, Neaşu IA, Pinheiro T, et al. Size-Dependent Biological Activities of Fluorescent Organosilane-Modified Zinc Oxide Nanoparticles. J Biomed Nanotechnol 2020;16:137–52. https://doi.org/10.1166/jbn.2020.2882.

44. Praseptiangga D, Zahara HL, Widjanarko PI, Made Joni I, Panatarani C. Preparation and FTIR spectroscopic studies of SiO2-ZnO nanoparticles suspension for the development of carrageenan-based bio-nanocomposite film. AIP Conf. Proc., vol. 2219, American Institute of Physics Inc.; 2020. https://doi.org/10.1063/5.0003434.
45. Moskowitz BM, Moon J, Li Y, Cheng Y, Daemen LL, Lee L, et al. Structure–Activity Relationships for Ethanol Dehydrogenation to Acetaldehyde by Silica-Supported Zinc Oxide Catalysts. ACS Catal 2025;15:17225–40. https://doi.org/10.1021/acscatal.5c03430.
46. Achehboune M, Khenfouch M, Boukhoubza I, Leontie L, Doroftei C, Carlescu A, et al. Microstructural, FTIR and Raman spectroscopic study of Rare earth doped ZnO nanostructures. Mater. Today Prc., vol. 53, Elsevier Ltd; 2021, p. 319–23. https://doi.org/10.1016/j.matpr.2021.04.144.
47. Atamnia K, Satha S, Satha H, Gonon MF. Synthesis, structural and thermal characterization of silica glasses containing BaO, SrO and ZnO oxides. Mater Res Express 2021;8. https://doi.org/10.1088/2053-1591/abd33c.
48. Serrano-Lotina A, Portela R, Baeza P, Alcolea-Rodriguez V, Villarroel M, Ávila P. Zeta potential as a tool for functional materials development. Catal Today 2023;423. https://doi.org/10.1016/j.cattod.2022.08.004.
49. Abouaitah K, Allayh AK, Wojnarowicz J, Shaker YM, Swiderska-Sroda A, Lojkowski W. Nanoformulation composed of ellagic acid and functionalized zinc oxide nanoparticles inactivates dna and rna viruses. Pharmaceutics 2021;13. https://doi.org/10.3390/pharmaceutics13122174.
50. Gudkov S V., Burmistrov DE, Serov DA, Rebezov MB, Semenova AA, Lisitsyn AB. A Mini Review of Antibacterial Properties of ZnO Nanoparticles. Front Phys 2021;9. https://doi.org/10.3389/fphy.2021.641481.
51. Ijaz M, Zafar M, Islam A, Afsheen S, Iqbal T. A Review on Antibacterial Properties of Biologically Synthesized Zinc Oxide Nanostructures. J Inorg Organomet Polym Mater 2020;30:2815–26. https://doi.org/10.1007/s10904-020-01603-9.
52. Batool M, Khurshid S, Qureshi Z, Daoush WM. Adsorption, antimicrobial and wound healing activities of biosynthesised zinc oxide nanoparticles. Chemical Papers 2021;75:893–907. https://doi.org/10.1007/s11696-020-01343-7.
53. Jamshidi D, Sazegar MR. Antibacterial activity of a novel biocomposite chitosan/graphite based on zinc-grafted mesoporous silica nanoparticles. Int J Nanomedicine 2020;15:871–83. https://doi.org/10.2147/IJN.S234043.
54. Klink MJ, Laloo N, Taka A, Pakade V, Monapathi M, Modise J. Synthesis, Characterization and Antimicrobial Activity of Zinc Oxide Nanoparticles against Selected Waterborne Bacterial and Yeast Pathogens. Molecules 2022;27. https://doi.org/10.3390/molecules27113532.
55. Jatrana I, Satiya H, Dwivedi P. Novel green synthesis of ZnO/SiO2nanocomposite: Characterization and biocidal activity. Mater. Today Proc., vol. 79, Elsevier Ltd; 2022, p. 148–54. https://doi.org/10.1016/j.matpr.2022.11.238.
56. Motelica L, Ficai D, Petrisor G, Oprea OC, Trușcă RD, Ficai A, et al. Antimicrobial Hydroxyethyl-Cellulose-Based Composite Films with Zinc Oxide and Mesoporous Silica Loaded with Cinnamon Essential Oil. Pharmaceutics 2024;16. https://doi.org/10.3390/pharmaceutics16091225.